Coexistence of antiferromagnetism and superconductivity within t-J model with strong correlations and nonzero spin polarization

Jan Kaczmarczyk*
Marian Smoluchowski Institute of Physics, Jagiellonian University, Reymonta 4, PL-30-059 Kraków, Poland

Jozef Spałek†
Marian Smoluchowski Institute of Physics, Jagiellonian University, Reymonta 4, PL-30-059 Kraków, Poland
Faculty of Physics and Applied Computer Science, AGH University of Science and Technology, Reymonta 19, PL-30-059 Kraków, Poland
(Received 14 June 2011; published 29 September 2011)

The coexistence of antiferromagnetism with superconductivity is studied theoretically within the t-J model with the Zeeman term included. The strong electron correlations are accounted for by means of the extended Gutzwiller projection method within a statistically consistent approach proposed recently. The phase diagram on the band filling-magnetic field plane is shown, and subsequently the system properties are analyzed for the fixed band filling $n = 0.97$. In this regime, the results reflect principal qualitative features observed recently in selected heavy-fermion systems, namely, (i) with the increasing magnetic field the system evolves from coexisting antiferromagnetic-superconducting phase through antiferromagnetic phase toward polarized paramagnetic state and (ii) the onset of superconducting order suppresses partly the staggered moment. The superconducting gap has both the spin-singlet and the staggered-triplet components, a direct consequence of a coexistence of the superconducting state with antiferromagnetism.

DOI: 10.1103/PhysRevB.84.125140 PACS number(s): 71.27.+a, 74.20.−z, 74.70.Tx, 74.25.Ha

I. INTRODUCTION

The interplay of antiferromagnetism (AF) with superconductivity (SC) is one of the important topics in condensed-matter physics,[1] as better understanding of this subject would improve our knowledge of a number of systems such as high-T_c,[2] heavy-fermion,[3] and organic[4] superconductors. In all those systems, superconductivity appears in the vicinity of magnetic phases (mostly antiferromagnetic but also ferromagnetic[5,6]). Moreover, magnetic interactions or fluctuations are very frequently considered to be the pairing mechanism in unconventional superconductors.[7–9] Typically, antiferromagnetism and superconductivity are competing quantum phenomena because of the competition between the Meissner-supercurrent screening and the internal-field generation by magnetic ordering. This antagonism can be overcome by a spatial separation of the AF and the SC phases or by subdivision of the f electrons into more localized (resulting in AF) and more itinerant (participating in SC) parts. However, especially interesting is the situation, when the same electrons are involved in both phenomena, as is the case for some heavy-fermion systems. There, SC and AF can coexist easily, when the periodicity of magnetic structure $\lambda_{\mathrm{AF}}(= 2a)$ is much smaller than the coherence length ξ for the Cooper pair. In other words, when $\xi \gg a$, the staggered exchange field averages out to zero within the coherence volume. In this respect, the Ce-based "115" heavy-fermion compounds—the family of CeMIn$_5$ (with M = Co,Rh,Ir[10–12])—is the most promising as both antiferromagnetism and superconductivity are believed to arise from $4f$ electrons, where even the interplay of the two orders can be studied by tuning the system with pressure, magnetic field, or doping.

Also, recently a competitive coexistence of AF and SC has been reported in both CeRhIn$_5$[13–16] and CeCo(In$_{1-x}$Cd$_x$)$_5$.[17,18] In the latter system, a mutual influence of AF and SC has been observed. Namely, it turns out that the onset of SC order with lowering temperature prevents any further increase of the antiferromagnetic magnetization.[17] A similar type of coexistence has also been observed in CeRhSi$_3$.[19]

Generally, in the heavy-fermion systems, strong correlations among electrons are the reason for an emergence of new and nontrivial physics. Those nontrivial features should be properly accounted for when modeling those systems. In the present paper, an investigation of the coexistence of AF with SC in an applied magnetic field is presented. To account for strong electron correlations, the Gutzwiller-projected t-J model is used with the Zeeman term included. The extended Gutzwiller scheme proposed recently[20] is utilized for calculation of statistical averages of the relevant operators. Our model, although at first sight seems too simplified to be related to heavy-fermion systems, it nonetheless reflects qualitatively principal features observed recently in selected heavy-fermion systems.

It is commonly believed that the minimal model for investigation of heavy-fermion systems should be the two-band periodic Anderson model (PAM) (see e.g., Ref. 21) or the Kondo lattice model.[22] On the other hand, the one-band calculations have already proved fruitful in the analysis of AF and SC coexistence in CeRhIn$_5$[23] as well as in investigations of the high-field low-temperature unconventional superconducting phase of CeCoIn$_5$.[24,25] The narrow-band limit of PAM has been discussed theoretically also elsewhere (see Refs. 26 and 27, Appendix A). Generally, it appears when only a single hybridized band is involved and in the heavy-fermion limit (i.e., when f-level occupancy $n_f = 1 - \delta$ with $\delta \ll 1$). Simply put, the t-J-type model reflects the physics of those hybridized and strongly correlated systems in the narrow f-band limit.

The paper is organized as follows. In Sec. II, we present the general theoretical formulation. In Sec. III, we show the

numerical results, and finally in Sec. IV, our findings are summarized and an outlook is provided.

II. MODEL, ORDER PARAMETERS, AND CONSTRAINTS

We start from the t-J model with the Zeeman term included, as represented by the Hamiltonian[28]

$$\hat{\mathcal{H}}_{tJ} = \hat{P}\left(\sum_{ij\sigma} t_{ij} c^{\dagger}_{i\sigma} c_{j\sigma} + J\sum_{\langle ij\rangle} \mathbf{S_i}\mathbf{S_j} - h\sum_{i\sigma}\sigma\hat{n}_{i\sigma}\right)\hat{P}, \quad (1)$$

where $\langle ij\rangle$ denotes the summation over bonds, and $\sigma = \pm 1$ is the spin z component. Since its derivation,[29,30] the t-J model represents an active field of research (see e.g., Ref. 31 for a recent analysis of the one-dimensional situation). The t-J model captures the essential ingredients of physics of the high-T_c superconductors. The advantage of using this model is that both AF and SC come from a microscopic parameter, antiferromagnetic exchange J, and therefore there are no phenomenological terms in the Hamiltonian (as opposed to some earlier studies of AF and SC coexistence). We neglect the orbital effects, as the Maki parameter[32] in the systems of our interest here is high.[15,33] The Gutzwiller projector $\hat{P} \equiv \Pi_i(1-\hat{n}_{i\uparrow}\hat{n}_{i\downarrow})$ eliminates double occupancies in real space. In the following, we will use the more general correlator

$$\hat{P}_C \equiv \Pi_i \lambda_{i\uparrow}^{\hat{n}_{i\uparrow}/2}\lambda_{i\downarrow}^{\hat{n}_{i\downarrow}/2}(1-\hat{n}_{i\uparrow}\hat{n}_{i\downarrow}), \quad (2)$$

where $\lambda_{i\sigma}$ are the so-called fugacity factors. Also, this correlator connects the correlated $|\Psi\rangle$ and uncorrelated $|\Psi_0\rangle$ wave functions[34] via

$$|\Psi\rangle = \hat{P}_C|\Psi_0\rangle. \quad (3)$$

This allows to express the average of any operator $\hat{O}$ in the correlated state as

$$\langle\hat{O}\rangle \equiv \langle\Psi|\hat{O}|\Psi\rangle = \frac{\langle\hat{P}_C\hat{O}\hat{P}_C\rangle_0}{\langle\hat{P}_C\hat{P}_C\rangle_0}, \quad (4)$$

where $\langle\ldots\rangle_0 \equiv \langle\Psi_0|\ldots|\Psi_0\rangle$. With the above equation one can in principle calculate the average value of Hamiltonian (1), namely,

$$W \equiv \langle\hat{\mathcal{H}}_{tJ}\rangle = \sum_{ij\sigma} t_{ij}\langle c^{\dagger}_{i\sigma}c_{j\sigma}\rangle + J\sum_{\langle ij\rangle}\left(\langle S^z_i S^z_j\rangle + \langle S^x_i S^x_j + S^y_i S^y_j\rangle\right) - h\sum_{i\sigma}\sigma\langle\hat{n}_{i\sigma}\rangle, \quad (5)$$

but this is a nontrivial task, since after applying the Wick theorem too many terms appear [see Ref. 20, e.g., Eq. (8) and the discussion afterwards], and one has to resort to making approximations at this point. There are a few ways to perform this operation, and this is still an active field of research, so one can expect new calculation schemes to appear.[35] Here, we use the scheme proposed recently by Fukushima[20,36] in the local-constraint version, which assumes that the average number of particles at any site and with any spin is unchanged by the projection,

$$\langle\hat{n}_{i\sigma}\rangle = \langle\hat{n}_{i\sigma}\rangle_0. \quad (6)$$

This formalism is known to reproduce the variational Monte Carlo results better than the conventional Gutzwiller approximation (at least, for the projected uniform nonmagnetic d-wave BCS superconductor—see Figs. 3 and 4 of Ref. 20). The local-constraint version of the formalism is quite general in the sense that it is capable of accounting for antiferromagnetism, superconductivity, and the ferromagnetic polarization. The explicit expressions for all averages appearing in Eq. (5) are given in Ref. 20. To express them in terms of mean fields of our interest, we need to assume what is the character of the uncorrelated wave function $|\Psi_0\rangle$. Since our goal is the description of coexistence of AF and SC, we assume the corresponding mean-fields as nonzero at the level of $|\Psi_0\rangle$ as in the following. We start with the particle number in the form

$$n_{i\sigma} \equiv \langle\hat{n}_{i\sigma}\rangle_0 = \tfrac{1}{2}(n + \sigma\, m_{\mathrm{FM}} + \sigma\, m_{\mathrm{AF}}\, e^{i\mathbf{Q}\cdot\mathbf{r_i}}), \quad (7)$$

where n is the band filling (assumed as constant), m_{FM} is the ferromagnetic (longitudinal) spin-polarization component, and m_{AF} is the antiferromagnetic (staggered) spin polarization. The factor $e^{i\mathbf{Q}\cdot\mathbf{r_i}}$ [with $\mathbf{Q} = (\pi,\pi)$] is responsible for the sign reversal of the staggered magnetic moment when exchanging the two sublattices A and B.[37] We also assume the superconducting order parameter can be decomposed into two components:

$$\Delta_{ij} \equiv \langle c_{j\downarrow}c_{i\uparrow}\rangle_0 = \begin{cases}\tau_{ij}\Delta_A, & \text{for } i \in \text{A sublattice},\\ \tau_{ij}\Delta_B, & \text{for } i \in \text{B sublattice},\end{cases} \quad (8)$$

where τ_{ij} ensures the d-wave gap symmetry by setting $\tau_{ij} = +1(-1)$ for $j = i \pm \hat{x}$ ($j = i \pm \hat{y}$), respectively, and with $\hat{x}$ and $\hat{y}$ being the square-lattice basis vectors. The d-wave solution (of the $d_{x^2-y^2}$ form) is taken throughout in the following analysis, as it is the most favorable energetically (cf. e.g., Ref. 38). The superconducting order parameter can be rewritten in terms of the singlet and the staggered π-triplet components, namely,

$$\begin{aligned}\Delta_{ij} &\equiv \langle c_{j\downarrow}c_{i\uparrow}\rangle_0\\ &\equiv \tfrac{1}{2}(\langle c_{j\downarrow}c_{i\uparrow} + c_{j\uparrow}c_{i\downarrow}\rangle_0 + \langle c_{j\downarrow}c_{i\uparrow} - c_{j\uparrow}c_{i\downarrow}\rangle_0)\\ &= \tfrac{1}{2}(\langle c_{j\downarrow}c_{i\uparrow} - c_{i\downarrow}c_{j\uparrow}\rangle_0 + \langle c_{j\downarrow}c_{i\uparrow} + c_{i\downarrow}c_{j\uparrow}\rangle_0)\\ &\equiv \Delta^{(S)}_{ij} + \Delta^{(T)}_{ij}\, e^{i\mathbf{Q}\cdot\mathbf{r_i}},\end{aligned} \quad (9)$$

with

$$\Delta^{(S)}_{ij} \equiv \tfrac{1}{2}\tau_{ij}(\Delta_A + \Delta_B), \quad (10)$$

$$\Delta^{(T)}_{ij} \equiv \tfrac{1}{2}\tau_{ij}(\Delta_A - \Delta_B). \quad (11)$$

The superconducting order parameter Δ_{ij} is defined on bond $\langle ij\rangle$ (nearest-neighbor pair of sites). To define the gap per site, we make use of the standard[39] relation for d-wave solution

$$\Delta^{(S)}_i \equiv \frac{1}{4}\sum_{j(i)}\tau_{ij}(\Delta_{i,j(i)} - \Delta_{j(i),i}) = \frac{1}{2}(\Delta_A + \Delta_B), \quad (12)$$

$$\Delta^{(T)}_i \equiv \frac{1}{4}\sum_{j(i)}\tau_{ij}(\Delta_{i,j(i)} + \Delta_{j(i),i}) = \frac{1}{2}(\Delta_A - \Delta_B)e^{i\mathbf{Q}\cdot\mathbf{r_i}}, \quad (13)$$

where $j(i)$ denotes the nearest neighbors of site i. The existence of the triplet component is inevitable even if there

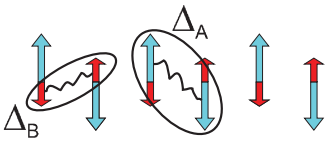

FIG. 1. (Color online) Spin-majority (blue, bigger arrows) and spin-minority (red, smaller arrows) electron spins in a system with the AF order and real-space superconducting gaps. Δ_A binds two spin-majority electrons, and Δ_B binds two spin-minority electrons and therefore there is a priori no reason for these two gaps to coincide (as would be the case for no staggered π-triplet component). In other words, the two distinct gaps make effectively the $\uparrow-\downarrow$ and $\downarrow-\uparrow$ pairing components of the opposite-spin pairs distinguishable.

is no triplet channel in the pairing potential. Namely, the triplet component is dynamically induced by the singlet gap and antiferromagnetism.[25,39–41] From a microscopic point of view, this is also not surprising at all (see Fig. 1 for an intuitive illustration). An interesting feature of the superconducting gap defined by Eq. (9) is the nonzero momentum of Cooper pairs for the triplet component [it results from the $e^{i\mathbf{Q}\cdot\mathbf{r}_i}$ term, in an analogy to center-of-mass momentum $\mathbf{Q}$ in the Fulde-Ferrell-Larkin-Ovchinnikov (FFLO) phase [42–44]]. A superconducting state with nonzero momentum has been investigated in a number of cases,[25,42,43,45] even in zero external magnetic field.[46,47] The one presented here is analogous to that from Ref. 25, except we consider both the microscopic (t-J) model and the limit of strong correlations.

With the above assumptions, we can express the ground-state energy W [cf. Eq. (5)] as a function of the band filling n, the magnetization components m_{FM} and m_{AF}, the superconducting gaps Δ_A and Δ_B, and the hopping amplitudes $\chi_{ij\sigma}\equiv\langle c^\dagger_{i\sigma}c_{j\sigma}\rangle_0$. We assume as nonzero the first- and second-nearest-neighbor hopping integrals t and t', which yields six different hopping amplitudes

$$\chi_{ij\sigma}\equiv\langle c^\dagger_{i\sigma}c_{j\sigma}\rangle_0\in\{\chi_{AB\uparrow},\chi_{AB\downarrow},\chi_{AA\uparrow},\chi_{AA\downarrow},\chi_{BB\uparrow},\chi_{BB\downarrow}\}. \tag{14}$$

The resulting expression for W is quite lengthy and has been presented in Appendix.

Next, as in the method proposed earlier[48–51] (our present formulation is analogous to that from Ref. 48), to solve the model in a statistically-consistent manner, we impose additionally the constraints on all introduced mean fields by means of the Lagrange multipliers method. In effect, to carry out the subsequent analysis, we use the following energy operator:

$$\begin{aligned}\hat{K}\equiv&-\sum_{ij\sigma}\left[\lambda^{(\chi)}_{ij\sigma}(c^\dagger_{i\sigma}c_{j\sigma}-\chi_{ij\sigma})+\mathrm{H.c.}\right]\\&-\sum_{ij}\left[\lambda^{(\Delta)}_{ij}(c_{j\downarrow}c_{i\uparrow}-\Delta_{ij})+\mathrm{H.c.}\right]\\&-\sum_{ij\sigma}\lambda^{(n)}_{i\sigma}(\hat{n}_{i\sigma}-n_{i\sigma})+W(n,m_{\mathrm{AF}},m_{\mathrm{FM}},\Delta_A,\Delta_B,\chi_{ij\sigma})\\&-\mu\sum_{i\sigma}\hat{n}_{i\sigma},\end{aligned} \tag{15}$$

where μ is the chemical potential.

This method of approach is equivalent in the $T\to\infty$ ($\beta\to 0$) limit to that presented in Refs. 52 and 53. The equivalence can be seen from the comparison of Eq. (15) and Eqs. (30)–(37) with the corresponding equations from Refs. 52 and 53 [e.g., Eq. (13) from Ref. 52 provides an effective Hamiltonian with the operator part equivalent to our $\hat{K}$]. The Lagrange multipliers $\lambda^{(\chi)}_{ij\sigma}$, $\lambda^{(\Delta)}_{ij}$, and $\lambda^{(n)}_{i\sigma}$ have the same symmetries, as the corresponding mean fields $\chi_{ij\sigma}$, Δ_{ij}, and $n_{i\sigma}$. We also assume they are spatially homogeneous. Namely,

$$\lambda^{(n)}_{i\sigma}\equiv\lambda_n+\sigma\lambda_{m_{\mathrm{FM}}}+\sigma\lambda_{m_{\mathrm{AF}}}e^{i\mathbf{Q}\cdot\mathbf{r}_i}, \tag{16}$$

$$\lambda^{(\Delta)}_{ij}\equiv\lambda^{(S)}_{\Delta}+\lambda^{(T)}_{\Delta}e^{i\mathbf{Q}\cdot\mathbf{r}_i}, \tag{17}$$

with

$$\lambda^{(S)}_{\Delta}=\tfrac{1}{2}(\lambda_{\Delta_A}+\lambda_{\Delta_B}), \tag{18}$$

$$\lambda^{(T)}_{\Delta}=\tfrac{1}{2}(\lambda_{\Delta_A}-\lambda_{\Delta_B}). \tag{19}$$

After performing Fourier transformation of the operator part of $\hat{K}$, we obtain

$$\begin{aligned}\hat{K}=&{\sum_{\mathbf{k}}}'\Psi^\dagger_{\mathbf{k}}\mathbf{M}_{\mathbf{k}}\Psi_{\mathbf{k}}+\Lambda(\mu+\lambda_n-\lambda_{m_{\mathrm{FM}}})+W(\vec{A})\\&+\Lambda\Big[n\lambda_n+m_{\mathrm{FM}}\lambda_{m_{\mathrm{FM}}}+m_{\mathrm{AF}}\lambda_{m_{\mathrm{AF}}}+4(\Delta_A\lambda_{\Delta_A}+\Delta_B\lambda_{\Delta_B})\\&+4\sum_{\sigma}(2\chi_{AB\sigma}\lambda_{\chi_{AB\sigma}}+\chi_{AA\sigma}\lambda_{\chi_{AA\sigma}}+\chi_{BB\sigma}\lambda_{\chi_{BB\sigma}})\Big],\end{aligned} \tag{20}$$

where the primed summation runs over the folded (magnetic) Brillouin zone, by $\vec{A}$ we denote all the mean-fields, Λ is the total number of sites, and the four-component operator $\Psi^\dagger_{\mathbf{k}}$ has the following components:

$$\Psi^\dagger_{\mathbf{k}}=(c^\dagger_{\mathbf{k}\uparrow},c_{-\mathbf{k}\downarrow},c^\dagger_{\mathbf{k}+\mathbf{Q}\uparrow},c_{-\mathbf{k}+\mathbf{Q}\downarrow}). \tag{21}$$

The matrix $\mathbf{M}_{\mathbf{k}}$ is given as

$$\mathbf{M}_{\mathbf{k}}=\begin{pmatrix}\xi_{\mathbf{k}\uparrow}&-2\lambda^{(S)}_{\Delta}\eta_{\mathbf{k}}&\zeta_{\mathbf{k}+\mathbf{Q}\uparrow}&-2\lambda^{(T)}_{\Delta}\eta_{\mathbf{k}+\mathbf{Q}}\\-2\lambda^{(S)}_{\Delta}\eta_{\mathbf{k}}&-\xi_{-\mathbf{k}\downarrow}&-2\lambda^{(T)}_{\Delta}\eta_{\mathbf{k}}&\zeta_{-\mathbf{k}\downarrow}\\\zeta_{\mathbf{k}\uparrow}&-2\lambda^{(T)}_{\Delta}\eta_{\mathbf{k}}&\xi_{\mathbf{k}+\mathbf{Q}\uparrow}&2\lambda^{(S)}_{\Delta}\eta_{\mathbf{k}+\mathbf{Q}}\\-2\lambda^{(T)}_{\Delta}\eta_{\mathbf{k}+\mathbf{Q}}&\zeta_{-\mathbf{k}+\mathbf{Q}\downarrow}&2\lambda^{(S)}_{\Delta}\eta_{\mathbf{k}+\mathbf{Q}}&-\xi_{-\mathbf{k}+\mathbf{Q}\downarrow}\end{pmatrix}, \tag{22}$$

where

$$\zeta_{\mathbf{k}\sigma} = -\sigma\,(\lambda_{\chi_{AA\sigma}} - \lambda_{\chi_{BB\sigma}})\epsilon'_{\mathbf{k}} - \lambda_{m_{\mathrm{AF}}}, \tag{23}$$

$$\xi_{\mathbf{k}\sigma} = -\mu - \lambda_n - \sigma\lambda_{m_{\mathrm{FM}}} - 2\epsilon_{\mathbf{k}}\lambda_{\chi_{AB\sigma}} - \epsilon'_{\mathbf{k}}(\lambda_{\chi_{AA\sigma}} + \lambda_{\chi_{BB\sigma}}), \tag{24}$$

$$\epsilon_{\mathbf{k}} = 2(\cos k_x + \cos k_y), \tag{25}$$

$$\epsilon'_{\mathbf{k}} = 4\cos k_x \cos k_y, \tag{26}$$

$$\eta_{\mathbf{k}} = \cos k_x - \cos k_y. \tag{27}$$

We have also used the fact that $\sum_{\mathbf{k}} \epsilon_{\mathbf{k}} = \sum_{\mathbf{k}} \epsilon'_{\mathbf{k}} = 0$. Note that in the present formulation $\lambda_{m_{\mathrm{FM}}}$ corresponds to sum of the magnetic field h and the correlation-induced field h_{cor}[54,55] (or equivalently the Lagrange multiplier β in the slave-boson theory[56–58]). Namely, $\lambda_{m_{\mathrm{FM}}} \equiv h + h_{\mathrm{cor}} \equiv h - \beta$, what is evident from comparison of Eq. (24) with appropriate expressions taken from Refs. 54–56.

Next, we determine the eigenvalues of $\mathbf{M}_{\mathbf{k}}$, as they correspond to quasiparticle excitations of the system. An analytic diagonalization of $\mathbf{M}_{\mathbf{k}}$ produces very long expressions, and more importantly, expressions with square roots of possibly negative numbers. Therefore, having in mind their subsequent implementation to calculate the physical properties, we diagonalize this matrix numerically. Next, having determined the eigenvalues $\{E_{\mathbf{k}i}\}_{i=1,2,3,4}$, we determine the generalized grand potential functional for the system of fermions, which is

$$\begin{aligned}\mathcal{F} = &-\beta^{-1} {\sum_{\mathbf{k},i=1,2,3,4}}' \ln(1 + e^{-\beta E_{\mathbf{k}i}}) + \Lambda(\mu + \lambda_n - \lambda_{m_{\mathrm{FM}}}) \\ &+ W(\vec{A}) + \Lambda\Big[n\lambda_n + m_{\mathrm{FM}}\lambda_{m_{\mathrm{FM}}} + m_{\mathrm{AF}}\lambda_{m_{\mathrm{AF}}} \\ &+ 4(\Delta_A\lambda_{\Delta_A} + \Delta_B\lambda_{\Delta_B}) \\ &+ 4\sum_{\sigma}(2\chi_{AB\sigma}\lambda_{\chi_{AB\sigma}} + \chi_{AA\sigma}\lambda_{\chi_{AA\sigma}} + \chi_{BB\sigma}\lambda_{\chi_{BB\sigma}})\Big].\end{aligned} \tag{28}$$

The physical (equilibrium) values of the mean fields and the Lagrange multipliers are obtained from the necessary conditions for $\mathcal{F}$ to have a minimum subject to the constraints, i.e.,

$$\frac{\partial\mathcal{F}}{\partial\vec{A}} = 0, \quad \frac{\partial\mathcal{F}}{\partial\vec{\lambda}} = 0, \tag{29}$$

where by $\vec{\lambda}$ we denote collectively the Lagrange multipliers. Equations $\partial\mathcal{F}/\partial\vec{A} = 0$ provide the explicit analytic expressions for the Lagrange multipliers, i.e.,

$$\lambda_n = -\Lambda^{-1}\partial_n W(\vec{A}), \tag{30}$$

$$\lambda_{m_{\mathrm{FM}}} = -\Lambda^{-1}\partial_{m_{\mathrm{FM}}} W(\vec{A}), \tag{31}$$

$$\lambda_{m_{\mathrm{AF}}} = -\Lambda^{-1}\partial_{m_{\mathrm{AF}}} W(\vec{A}), \tag{32}$$

$$\lambda_{\Delta_A} = -\tfrac{1}{4}\Lambda^{-1}\partial_{\Delta_A} W(\vec{A}), \tag{33}$$

$$\lambda_{\Delta_B} = -\tfrac{1}{4}\Lambda^{-1}\partial_{\Delta_B} W(\vec{A}), \tag{34}$$

$$\lambda_{\chi_{AB\sigma}} = -\tfrac{1}{8}\Lambda^{-1}\partial_{\chi_{AB\sigma}} W(\vec{A}), \tag{35}$$

$$\lambda_{\chi_{AA\sigma}} = -\tfrac{1}{4}\Lambda^{-1}\partial_{\chi_{AA\sigma}} W(\vec{A}), \tag{36}$$

$$\lambda_{\chi_{BB\sigma}} = -\tfrac{1}{4}\Lambda^{-1}\partial_{\chi_{BB\sigma}} W(\vec{A}). \tag{37}$$

The above expressions can be utilized to eliminate Lagrange multipliers $\vec{\lambda}$ from the solution procedure. Thus we obtain 11 equations to be solved numerically for the mean fields $\vec{A}$, instead of 22 equations for both $\vec{A}$ and $\vec{\lambda}$. The equations for the mean fields (obtained from $\partial\mathcal{F}/\partial\vec{\lambda} = 0$) have the following form:

$$0 = \beta^{-1}\partial_{\lambda_n} f_\beta(\vec{\lambda}) - \Lambda(n-1), \tag{38}$$

$$0 = \beta^{-1}\partial_{\lambda_{m_{\mathrm{FM}}}} f_\beta(\vec{\lambda}) - \Lambda(m_{\mathrm{FM}} + 1), \tag{39}$$

$$0 = \beta^{-1}\partial_{\lambda_{m_{\mathrm{AF}}}} f_\beta(\vec{\lambda}) - \Lambda m_{\mathrm{AM}}, \tag{40}$$

$$0 = \beta^{-1}\partial_{\lambda_{\Delta_A}} f_\beta(\vec{\lambda}) - 4\Lambda\Delta_A, \tag{41}$$

$$0 = \beta^{-1}\partial_{\lambda_{\Delta_B}} f_\beta(\vec{\lambda}) - 4\Lambda\Delta_B, \tag{42}$$

$$0 = \beta^{-1}\partial_{\lambda_{\chi_{AB\sigma}}} f_\beta(\vec{\lambda}) - 8\Lambda\chi_{AB\sigma}, \tag{43}$$

$$0 = \beta^{-1}\partial_{\lambda_{\chi_{AA\sigma}}} f_\beta(\vec{\lambda}) - 4\Lambda\chi_{AA\sigma}, \tag{44}$$

$$0 = \beta^{-1}\partial_{\lambda_{\chi_{BB\sigma}}} f_\beta(\vec{\lambda}) - 4\Lambda\chi_{BB\sigma}, \tag{45}$$

where

$$f_\beta(\vec{\lambda}) \equiv {\sum_{\mathbf{k},i=1..4}}' \ln(1 + e^{-\beta E_{\mathbf{k}i}}). \tag{46}$$

The derivatives $\partial_\lambda f_\beta(\vec{\lambda})$ are computed numerically with a 5-point stencil method (as it gives two-three orders of magnitude better precision than the standard 3-point stencil). For example,

$$\begin{aligned}\partial_{\lambda_n} f_\beta(\vec{\lambda}) = \frac{1}{12x}[&-f_\beta(\lambda_n + 2x, \lambda_{m\mathrm{FM}}, \lambda_{m\mathrm{AF}}, \ldots) \\ &+ 8f_\beta(\lambda_n + x, \lambda_{m\mathrm{FM}}, \lambda_{m\mathrm{AF}}, \ldots) \\ &- 8f_\beta(\lambda_n - x, \lambda_{m\mathrm{FM}}, \lambda_{m\mathrm{AF}}, \ldots) \\ &+ f_\beta(\lambda_n - 2x, \lambda_{m\mathrm{FM}}, \lambda_{m\mathrm{AF}}, \ldots)] \\ &+ \mathrm{O}(x^4),\end{aligned} \tag{47}$$

where we use the "equilibrium" values of $\vec{\lambda}$ as given by Eqs. (30)–(37). The step x is typically equal to $x = 0.0001$. Larger values of x would cause greater error in the above formula. Smaller values would result in a loss of numerical precision. We have verified that at $h = 0$ (where analytical formulas for the eigenvalues $E_{\mathbf{k}i}$ are available) the numerical computation of the derivatives according to Eq. (47) with the chosen step $x = 0.0001$ introduces error smaller than the precision of the procedure of solving the set of Eqs. (38)–(45). The value of the step x has been chosen after an analysis of the error at $h = 0$ and the numerical-precision loss [for very small x the numerical-precision loss leads to impossibility of solving the set of Eqs. (38)–(45) with the given precision].

III. RESULTS AND PHYSICAL DISCUSSION

Equations (38)–(45) are solved numerically with the use of GNU Scientific Library (GSL)[59] on a grid of size $\Lambda = 256 \times 256$. We use the GSL-MULTIROOT-FSOLVER-HYBRIDS solver, which implements the hybrids algorithm. We use the precision $epsabs = 10^{-7}$. Namely, the procedure converges when the relation $\sum_i |f_i| < epsabs$ is fulfilled (where the sum is taken over all equations, which have been brought to the form $f_i = 0$ and divided by Λ to ensure lattice-independent convergence conditions). We assume the following values of parameters: $t = 3$, $t' = t/4 = 0.75$, $J = 1$, and $\beta = 500$, what yields the temperature $T = 1/\beta = 0.002 \approx 0$. In Table I, the exemplary numerical values of the parameters have been

TABLE I. Equilibrium values of mean-field variables, Lagrange multipliers, free energy F, and grand potential functional $\mathcal{F}$ at $n = 0.97$, $h = 0.3$, and $\beta = 500$.

Variable	Value	Variable	Value
μ	3.299 7360	λ_n	−5.133 1996
m_{FM}	0.000 0000	$\lambda_{m_{\mathrm{FM}}}$	0.300 0001
m_{AF}	0.810 0315	$\lambda_{m_{\mathrm{AF}}}$	2.581 7963
Δ_A	0.092 2998	λ_{Δ_A}	0.273 0140
Δ_B	0.047 9298	λ_{Δ_B}	0.439 5630
$\chi_{AB\uparrow}$	0.121 8625	$\lambda_{\chi_{AB\uparrow}}$	0.425 8402
$\chi_{AB\downarrow}$	0.121 8625	$\lambda_{\chi_{AB\downarrow}}$	0.425 8402
$\chi_{AA\uparrow}$	−0.016 7505	$\lambda_{\chi_{AA\uparrow}}$	−0.103 1297
$\chi_{AA\downarrow}$	0.027 5895	$\lambda_{\chi_{AA\downarrow}}$	−0.012 0561
$\chi_{BB\uparrow}$	0.027 5895	$\lambda_{\chi_{BB\uparrow}}$	−0.012 0561
$\chi_{BB\downarrow}$	−0.016 7505	$\lambda_{\chi_{BB\downarrow}}$	−0.103 1297
F/Λ	−1.011 0048	$\mathcal{F}/\Lambda$	−4.211 7488

provided for the sake of completeness. Numerical accuracy is on the level of the last digit specified. The energy scale has been set by taking the value of the exchange integral as unit, $J = 1$. For more details on the numerical procedure see Chap. 6 of Ref. 60.

A number of stable phases emerge as solutions of the equations, depending on the physical condition (n, h). As we work with constant number of particles n, the stable phase is the one with the lowest free energy, defined by

$$F = \mathcal{F}_0 + \mu n \Lambda, \tag{48}$$

where all the optimal values of mean fields and Lagrange multipliers [i.e., those being solution to Eqs. (30)–(45)] are inserted in the functional $\mathcal{F}$.

The exemplary phase diagram on the band filling n-magnetic field h plane is exhibited in Fig. 2. It can be seen that the antiferromagnetic phase is the predominant one in the low-field regime and above $n = 0.8$. For $n \gtrsim 0.935$, antiferromagnetism coexists with superconductivity, what amounts to a phase with nonzero three order parameters (similarly, as in e.g., Ref. 25). In the low-n part of the phase diagram (for $n < 0.8$), the saturated ferromagnetic (SFM) phase with $m_{\mathrm{FM}} = n$ becomes the stable state. This phase is stable even in the $h \to 0$ limit. This is an interesting result, which adds to the discussion of ferromagnetism in the t-J[61–63] model. There is also a number of papers (see e.g., Refs. 48 and 64) analyzing the t-J model (1) with the Gutzwiller-type of approach with the parameters in a similar range (i.e., with $n < 0.8$ and similar values of t_{ij} and J). Some of those papers disregard completely the Zeeman-term influence, and this omission is justified when applying the model to high-T_c superconductors, where orbital effects dominate over the Pauli magnetism. We have shown, that even at $h = 0$ the system may be completely spin-polarized and therefore the inclusion of ferromagnetic polarization m_{FM} is important in the treatment of the t-J model. Finally, our phase diagram can be compared (although this is not a direct comparison, as even at $h = 0$ we have $m_{\mathrm{FM}} \neq 0$ for the AF phase) to that obtained by another Gutzwiller approximation scheme[65] in which the coexisting phase was stable up to the doping $\delta \equiv 1 - n = 0.1$, and for higher doping levels the pure superconducting state was stable. In our approach, the antiferromagnetic phase is stable for such dopings instead. We comment on the strong antiferromagnetism in the following analysis.

At band filling $n = 0.97$, the phase diagram (or the phase sequence as a function of field h) resembles those observed recently in the heavy-fermion compounds $CeCo(In_{1-x}Cd_x)_5$[17] at doping $x = 0.0075$ and $CeRhSi_3$[19] at pressure $p \approx 17$ kbar.[66] Namely, in low magnetic fields, a phase with coexisting antiferromagnetic and superconducting orders (AF + SC) is stable,

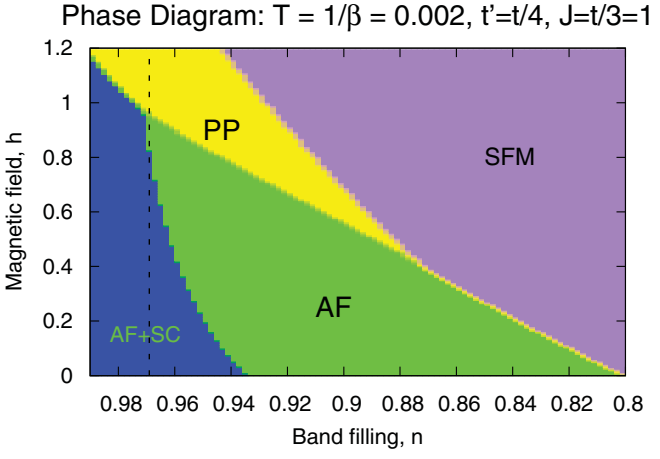

FIG. 2. (Color online) Phase diagram on the band filling-magnetic field plane. The phases are labeled as follows: AF + SC-phase with coexisting superconductivity and antiferromagnetism, AF—antiferromagnetic phase, PP—polarized paramagnetic phase, and SFM—saturated ferromagnetic phase (with $m_{\mathrm{FM}} = n$). No stable pure superconducting solution has been found. For a further analysis, we restrict ourselves to $n = 0.97$ as marked by the dashed vertical line.

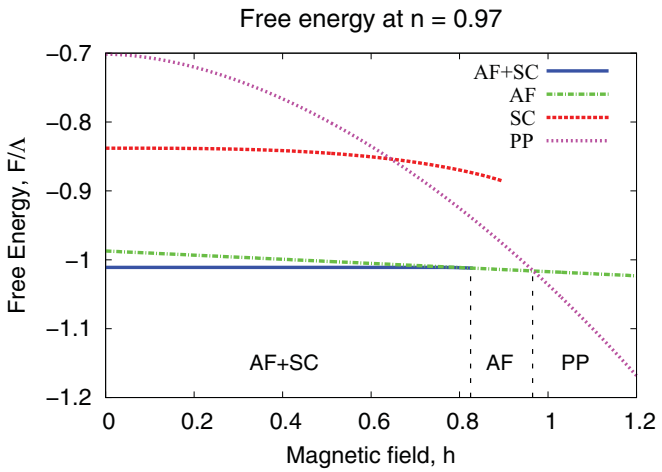

FIG. 3. (Color online) Free energy per site as a function of magnetic field for the specified selection of phases. Types of order are marked explicitly at the bottom. The "SC" phase is the pure superconducting phase (i.e., with $m_{\mathrm{AF}} = 0$), which obviously has higher energy than other phases and hence does not appear in the phase diagram. The vertical dashed lines mark the phase boundaries: the (AF + SC)-AF line marks a continuous transition, whereas that for the AF-PP is discontinuous, as one can see by looking at the behavior of the slope $\partial F/\partial h$.

whereas for higher magnetic fields a continuous transition to a pure antiferromagnetic (AF) phase takes place, followed by a discontinuous transition to the polarized paramagnetic (PP) phase. The phases appearing at this band filling ($n = 0.97$) are analyzed thus in detail in the following.

In Fig. 3, we have plotted the free-energy curves for a choice of possible *a priori* phases. It can be seen (also from the following figures) that the transition AF + SC $\rightarrow$ AF is continuous, whereas the transition AF $\rightarrow$ PP is of the first order. Also, the pure superconducting (SC) solution is unstable, and this holds for other band fillings as well. It can be concluded from Fig. 3 that antiferromagnetism is the "dominating" phenomenon, since the energy gain from developing antiferromagnetic order (which can be seen from a closer look at the difference $F_{PP} - F_{AF}$) is much higher than the gain from developing superconducting order ($F_{PP} - F_{SC}$). Moreover, the energy gain from developing AF order within the SC phase ($F_{SC} - F_{AF+SC}$) is much higher than that from developing SC order within the AF phase ($F_{AF} - F_{AF+SC}$). This observation can be compared to the results of the

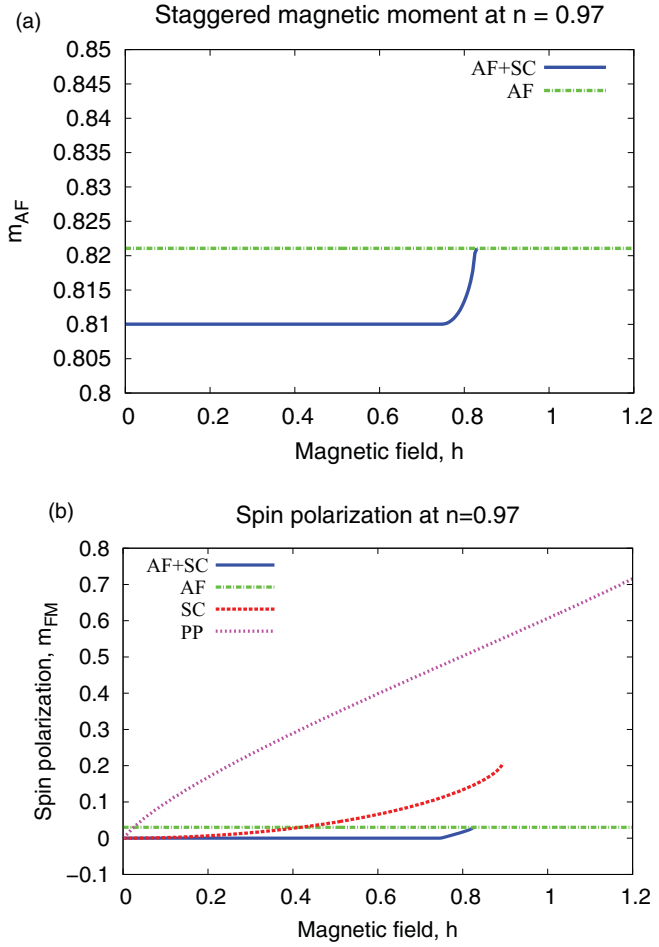

FIG. 4. (Color online) Staggered magnetic moment (a) and ferromagnetic spin polarization (b) for the selected phases. Obviously, the staggered moment of the SC and PP phases is zero and has not been plotted in (a). The magnetic moment value is insensitive to the projection (i.e., it is the same in both the correlated $|\Psi\rangle$ and the uncorrelated $|\Psi_0\rangle$ states).

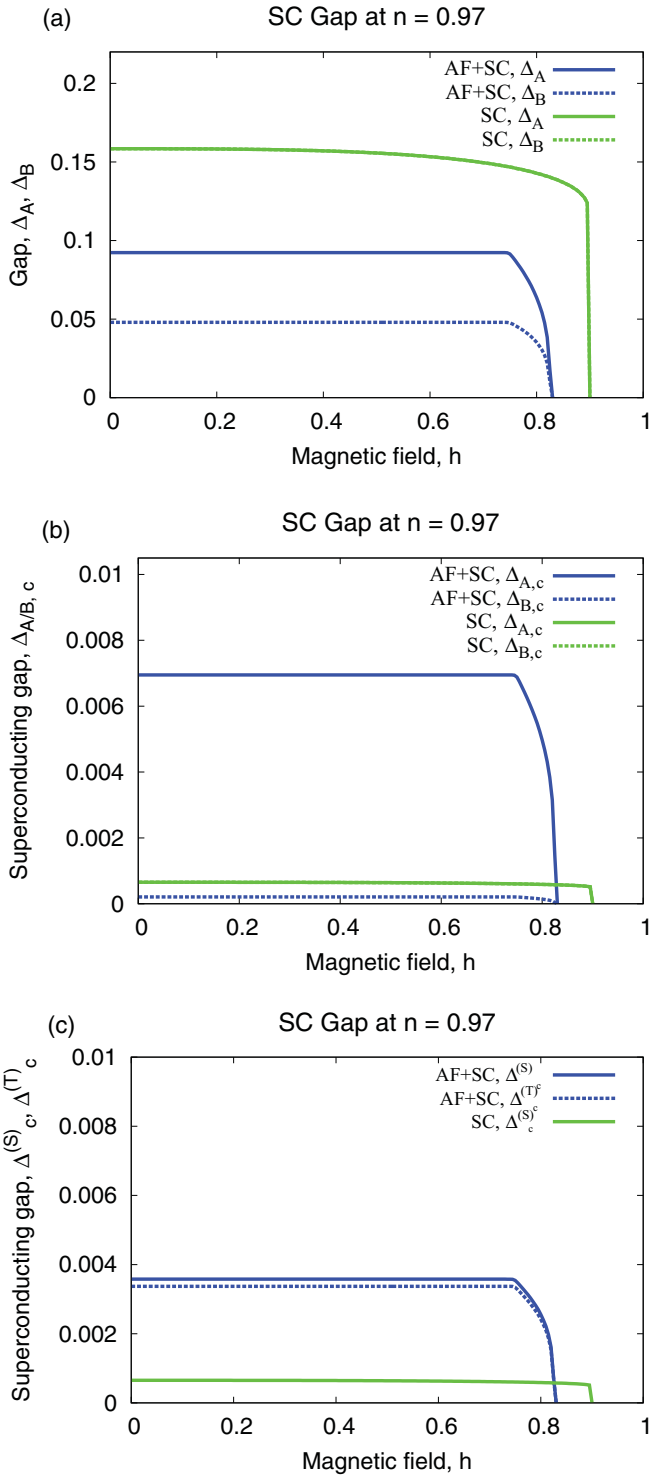

FIG. 5. (Color online) Superconducting gaps vs magnetic field for AF + SC and SC phases. (a) Δ_A and Δ_B gaps obtained for the uncorrelated wave function $|\Psi_0\rangle$; (b) and (c) gaps for the state specified by the correlated wave function (labeled as Δ_c), as given by Eq. (4). (b) shows the sublattice-specific Δ_A and Δ_B gaps, and (c) shows the singlet and triplet components of the gap. Note that the superconducting gaps (Δ_c) are enhanced in the AF + SC state (with respect to that in the pure SC state, which is however an unstable state). Also, the singlet and the staggered-triplet components are almost equal in the correlated state.

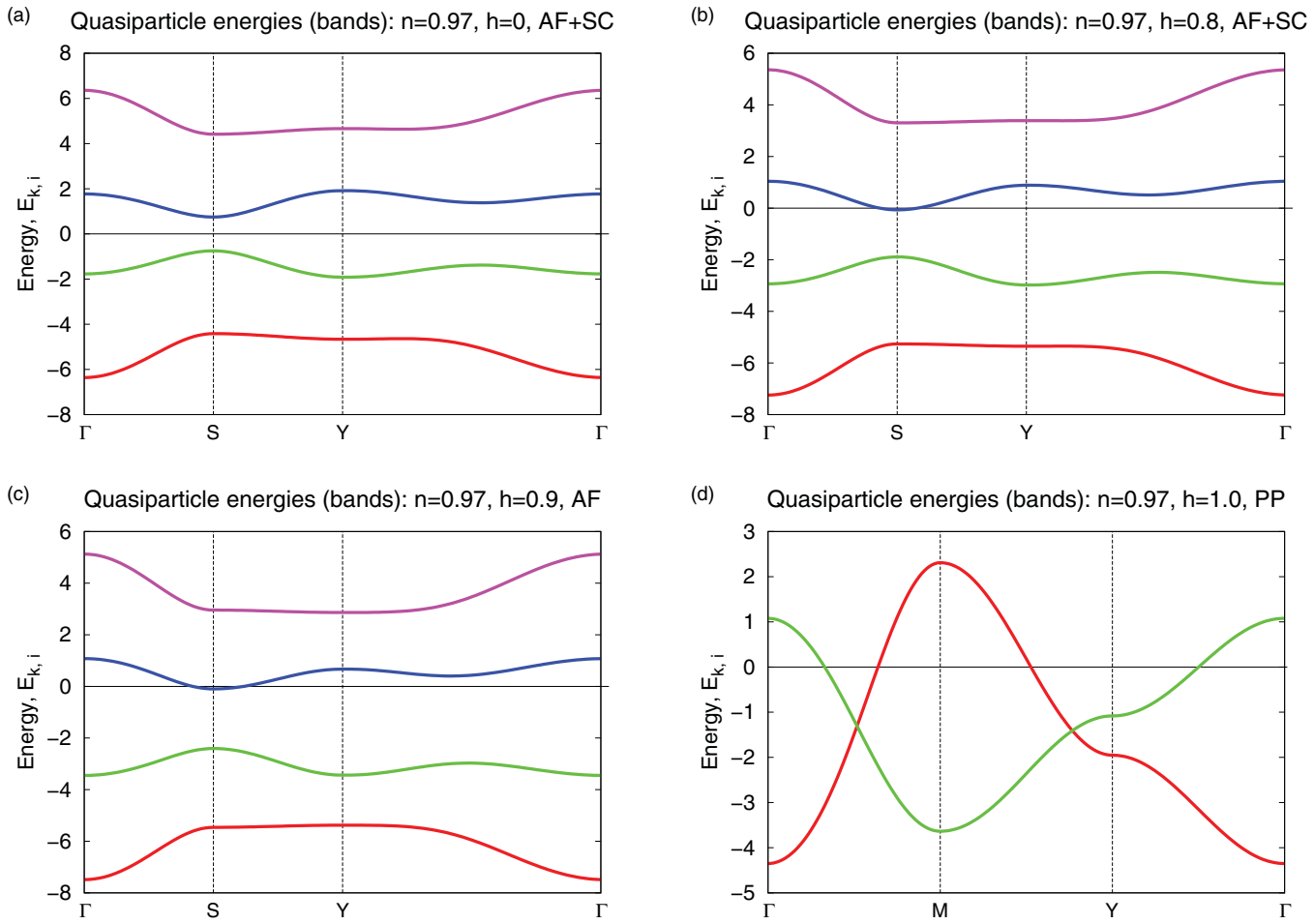

FIG. 6. (Color online) Quasiparticle energies (bands) for phases obtained at $n = 0.97$: (a) AF + SC phase ($h = 0$), (b) AF + SC phase with nonzero spin polarization ($h > 0$), (c) AF phase, and (d) PP phase (for a different path in the Brillouin zone). The full Brillouin zone (d) is spanned by the vertices $(\pm\pi, \pm\pi)$, whereas the folded (magnetic) Brillouin zone (a)–(c), by $(\pm\pi,0)$ and $(0, \pm\pi)$. The characteristic points are the following: $\Gamma = (0,0)$, $S = (\pi/2,\pi/2)$, $Y = (0,\pi)$, and $M = (\pi,\pi)$. Note that in (a)–(c) two of the energies $E_{\mathbf{k}i}$ (those with $E_{\mathbf{k}i} > 0$) describe quasiparticle states, and the other two represent quasihole states. Also, in (d) only two energies are displayed, as the Brillouin zone is not the folded (magnetic) one but the full Brillouin zone, because there is no antiferromagnetism in this case. The red (dark) curve in (d) describes a quasiparticle with $\sigma =\uparrow$, and the green (light) curve describes a quasihole with $\sigma =\downarrow$. The fully gapped electronic structure in (a)–(c) is caused by the magnetic (renormalized Slater) gap appearance in the AF + SC and the AF phases. Energy scale is in units of J.

variational Monte Carlo method,[67] in which the d-wave solution is only slightly higher in energy than the coexisting phase [see Fig. 2 of Ref. 67].

In Fig. 4, we exhibit the magnetic moment per site of the system for different phases. Namely, we plot the staggered magnetization m_{AF} and the ferromagnetic magnetization m_{FM} (spin polarization). The staggered magnetization is close to the saturation value of $m_{\mathrm{AF}} = n = 0.97$. Such overestimation of the staggered magnetization value over the variational Monte Carlo results[67,68] is also present in the slave-boson approach.[69] This is not surprising, as the method we use[48–51] is similar in structure (the Lagrange multipliers are present in both methods) to the slave-bosons approach (for the discussion of the equivalence for the paramagnetic state see Ref. 51). The obtained ferromagnetic spin polarization for the pure AF phase is equal to $m_{\mathrm{FM}} = 1 - n$ at all magnetic fields. Also, it can be seen that development of the SC order within the AF phase alters by a small amount the staggered magnetization m_{AF}, which drops by approximately 1% [see Fig. 4(a)].

In Fig. 5, various superconducting gaps are shown. Namely we exhibit both the "uncorrelated" gap for the wave function $|\Psi_0\rangle$ as well as the gap for the correlated wave function $|\Psi\rangle$, the latter defined by Eq. (4) and labeled as Δ_c. In the pure SC phase, the sublattice gaps are equal ($\Delta_A = \Delta_B$), which amounts to the absence of the triplet component. Note that although the uncorrelated gaps (Δ_A, Δ_B) are larger in the pure SC phase than in the AF + SC phase, the correlated gaps ($\Delta_c^{(S)}$, $\Delta_c^{(T)}$) are much larger in the AF + SC phase than in the pure SC phase. This very important conclusion means that the presence of antiferromagnetism supports superconductivity in the present situation. The opposite is not true as the staggered moment is slightly larger in the AF phase than in the AF + SC phase. Finally, the renormalized gaps are more than an order of magnitude smaller than their bare (uncorrelated) correspondents.

The picture with large antiferromagnetic magnetization m_{AF} (Fig. 4) and small superconducting gap (see Fig. 5) is consistent with the energy curves displayed in Fig. 3. To shift the energy balance toward the SC phase, one could either decrease t' or increase J. By doing that within a wide parameter margin, the antiferromagnetic phase still remains a predominant phase. Another possibility to weaken antiferromagnetism is to include additionally the intersite attraction ($V\sum_{\langle ij\rangle}\hat{n}_i\hat{n}_j$) in the starting Hamiltonian. This has been shown to stabilize the d-wave superconducting state[24] (see Ref. 36 for the expression for the average value of this term within the extended Gutzwiller scheme we use). The strong antiferromagnetism may represent an apparent feature of the Gutzwiller scheme used[20] in which magnetization is not changed by the projection, as follows directly from Eq. (6).

Finally, in Fig. 6, we display the quasiparticle energies (the Slater subbands) for the phases discussed above for $n = 0.97$. The crossing of one of the bands with the zero-energy line at the S point of the Brillouin zone in Figs. 6(b) and 6(c) means that the quasiparticle excitations will be spontaneously created (are gapless), a circumstance leading to a nonzero spin polarization (cf. Fig. 6), similarly as in the situation for the FFLO state.[42] Note also that for $h = 0$ the AF + SC electronic structure is gapful for the d-wave superconducting phase, because of the presence of the isotropic Slater-type (magnetic) splitting. This is not true anymore for $h \gtrsim 0.8$ [cf. Figs. 6(b), 6(c), and 4(b)] when a uniform ferromagnetic component appears. Also, the bands are sizably wider in the polarized paramagnetic state.

IV. SUMMARY

In summary, we have carried out a detailed analysis of the coexistence of antiferromagnetism and superconductivity within a microscopic t-J model with the Zeeman term included. The strong correlations were accounted for by means of the extended Gutzwiller projection method. Also, the constraints assuring the statistical consistency of the results have been included. We have obtained the phase diagram on the band filling-magnetic field plane, in which for the band fillings in the range $n \approx 0.935$–0.970 and with the increasing magnetic field, a series of phase transitions takes place. Namely, the system evolves from the coexisting AF + SC phase, through the antiferromagnetic (AF) phase, to the polarized paramagnetic (PP) phase. Also, the onset of superconducting order reduces the AF order parameter. By contrast, the superconducting gaps are enhanced by the presence of the AF order. In the AF + SC phase there are two superconducting gaps of an almost equal amplitude: the singlet and the staggered-triplet components. These features reflect in a qualitative manner the experimental findings in the $CeCo(In_{1-x}Cd_x)_5$[17,18] and $CeRhSi_3$[19] heavy-fermion systems, although our model is too simplified to be quantitatively related to such complex heavy-fermion systems. Additionally, both antiferromagnetism and superconductivity originate from the same electrons and are driven by the same kinetic-exchange interaction. Note that the real-space pairing is the pairing without "boson glue," i.e., without *paramagnons*. It is the mechanism of pairing arising entirely from interelectron correlations that is particularly effective when renormalized hopping and exchange interaction are of comparable magnitude.

As mentioned earlier, it would be very interesting to perform similar analysis within the periodic Anderson model, as this might allow for a comparison with the experiments (work along this line is in progress in our group[70]). Also, testing other Gutzwiller schemes seems crucial to verify if the strong antiferromagnetism and the tendency toward saturated ferromagnetism are only the characteristic features of the utilized renormalization scheme, or represent a universal tendency of the projected t-J model. For that purpose, the inclusion of realistic, orbitally degenerate f level structure, not just pseudospin Γ_7 doublet of Ce^{3+}, would be desirable.

One should also note that the present approach includes the effect of applied magnetic field only via the Zeeman term (the Pauli limit). For discussion of high-temperature superconductivity for $h > 0$, the orbital effects should be incorporated.

ACKNOWLEDGMENTS

The work was supported by Ministry of Science and Higher Education, Grant Nos. N N202 173735 and N N202 128736 as well as by the Foundation for Polish Science under the "TEAM" program for the years 2011–2014. Discussions with Olga Howczak and Jakub Jędrak are appreciated.

APPENDIX: EXPLICIT EXPRESSION FOR W

We provide here the expression for $W \equiv \langle \hat{\mathcal{H}}_{tJ}\rangle$. This expression can be divided into parts coming from different terms of Hamiltonian with $W_t \equiv \sum_{ij\sigma} t_{ij}\langle c^{\dagger}_{i\sigma}c_{j\sigma}\rangle$ and $W_J \equiv J\sum_{\langle ij\rangle}(\langle S^z_i S^z_j\rangle + \langle S^x_i S^x_j + S^y_i S^y_j\rangle)$, as follows, $W = W_t + W_J - \Lambda h m_{\mathrm{FM}}$. The expressions for W_J and W_t are given by

$$
\begin{aligned}
W_J = 2J\Lambda\Bigg[& -\frac{4(\chi_{AB\downarrow}\chi_{AB\uparrow}+\Delta_A\Delta_B)}{\sqrt{m_{\mathrm{AF}}^4+\left[m_{\mathrm{FM}}^2-(-2+n)^2\right]^2-2m_{\mathrm{AF}}^2\left[m_{\mathrm{FM}}^2+(-2+n)^2\right]}}+\frac{1}{4}\big((-m_{\mathrm{AF}}+m_{\mathrm{FM}})(m_{\mathrm{AF}}+m_{\mathrm{FM}}) \\
& -\big\{4\big[\Delta_A^2(-1+m_{\mathrm{AF}}-m_{\mathrm{FM}})(-1+m_{\mathrm{AF}}+m_{\mathrm{FM}})(2+m_{\mathrm{AF}}-m_{\mathrm{FM}}-n)(2+m_{\mathrm{AF}}+m_{\mathrm{FM}}-n) \\
& +\chi_{AB\uparrow}^2(1+m_{\mathrm{AF}}-m_{\mathrm{FM}})(-1+m_{\mathrm{AF}}+m_{\mathrm{FM}})(2+m_{\mathrm{AF}}+m_{\mathrm{FM}}-n)(-2+m_{\mathrm{AF}}-m_{\mathrm{FM}}+n) \\
& +\chi_{AB\downarrow}^2(-1+m_{\mathrm{AF}}-m_{\mathrm{FM}})(1+m_{\mathrm{AF}}+m_{\mathrm{FM}})(2+m_{\mathrm{AF}}-m_{\mathrm{FM}}-n)(-2+m_{\mathrm{AF}}+m_{\mathrm{FM}}+n) \\
& +\Delta_B^2(1+m_{\mathrm{AF}}-m_{\mathrm{FM}})(1+m_{\mathrm{AF}}+m_{\mathrm{FM}})(-2+m_{\mathrm{AF}}-m_{\mathrm{FM}}+n)(-2+m_{\mathrm{AF}}+m_{\mathrm{FM}}+n)\big]\big\} \\
& /[(2+m_{\mathrm{AF}}-m_{\mathrm{FM}}-n)(2+m_{\mathrm{AF}}+m_{\mathrm{FM}}-n)(-2+m_{\mathrm{AF}}-m_{\mathrm{FM}}+n)(-2+m_{\mathrm{AF}}+m_{\mathrm{FM}}+n)]\big)\Bigg],
\end{aligned}
\tag{A1}
$$

and

$$
\begin{aligned}
W_t = 2\Lambda\Bigg[& -4(1-n)\Bigg\{\frac{4\chi_{AB\downarrow}\Delta_A\Delta_B+\chi_{AB\uparrow}\left[4\chi_{AB\downarrow}^2+m_{\mathrm{AF}}^2-(2+m_{\mathrm{FM}}-n)^2\right]}{\left[m_{\mathrm{AF}}^2-(2+m_{\mathrm{FM}}-n)^2\right]\sqrt{-m_{\mathrm{AF}}^2+(-2+m_{\mathrm{FM}}+n)^2}} \\
& +\frac{4\chi_{AB\uparrow}\Delta_A\Delta_B+\chi_{AB\downarrow}\left[4\chi_{AB\uparrow}^2+m_{\mathrm{AF}}^2-(-2+m_{\mathrm{FM}}+n)^2\right]}{\sqrt{-m_{\mathrm{AF}}^2+(2+m_{\mathrm{FM}}-n)^2}\left[m_{\mathrm{AF}}^2-(-2+m_{\mathrm{FM}}+n)^2\right]}\Bigg\}t \\
& +\Bigg(2(-1+n)-\frac{\left\{\chi_{BB\uparrow}\left[-4\chi_{BB\downarrow}^2+(-2+m_{\mathrm{AF}}-m_{\mathrm{FM}}+n)^2\right]\right\}}{(2+m_{\mathrm{AF}}-m_{\mathrm{FM}}-n)} \\
& +\frac{\chi_{BB\downarrow}(-2+m_{\mathrm{AF}}-m_{\mathrm{FM}}+n)\left[-4\chi_{BB\uparrow}^2+(-2-m_{\mathrm{AF}}+m_{\mathrm{FM}}+n)^2\right]^2}{-2-m_{\mathrm{AF}}+m_{\mathrm{FM}}+n}\Bigg)t'\Bigg]\Bigg/(-2+m_{\mathrm{AF}}-m_{\mathrm{FM}}+n)^2 \\
& +\big(2(-1+n)\big\{\chi_{AA\uparrow}\left[-4\chi_{AA\downarrow}^2+(2+m_{\mathrm{AF}}+m_{\mathrm{FM}}-n)^2\right](-2+m_{\mathrm{AF}}+m_{\mathrm{FM}}+n) \\
& -\chi_{AA\downarrow}(2+m_{\mathrm{AF}}+m_{\mathrm{FM}}-n)\left[-4\chi_{AA\uparrow}^2+(-2+m_{\mathrm{AF}}+m_{\mathrm{FM}}+n)^2\right]\big\}\,t'\big) \\
& /[(2+m_{\mathrm{AF}}+m_{\mathrm{FM}}-n)^2(-2+m_{\mathrm{AF}}+m_{\mathrm{FM}}+n)^2]. \qquad \text{(A2)}
\end{aligned}
$$

*jan.kaczmarczyk@uj.edu.pl
†ufspalek@if.uj.edu.pl

[1] E. Demler, W. Hanke, and S.-C. Zhang, Rev. Mod. Phys. **76**, 909 (2004).
[2] P. A. Lee, N. Nagaosa, and X.-G. Wen, Rev. Mod. Phys. **78**, 17 (2006).
[3] C. Pfleiderer, Rev. Mod. Phys. **81**, 1551 (2009).
[4] J. Wosnitza, J. Low Temp. Phys. **146**, 641 (2007).
[5] S. Saxena, P. Agarwal, K. Ahilan, F. Grosche, R. Haselwimmer, M. Steiner, E. Pugh, I. Walker, S. Julian, P. Monthoux, G. Lonzarich, A. Huxley, I. Sheikin, D. Braithwaite, and J. Flouquet, Nature (London) **406**, 587 (2000).
[6] D. Aoki, A. Huxley, E. Ressouche, D. Braithwaite, J. Flouquet, J.-P. Brison, E. Lhotel, and C. Paulsen, Nature (London) **413**, 613 (2001).
[7] P. Monthoux, D. Pines, and G. Lonzarich, Nature (London) **450**, 1177 (2007).
[8] P. Monthoux and G. G. Lonzarich, Phys. Rev. B **59**, 14598 (1999).
[9] P. Monthoux and G. G. Lonzarich, Phys. Rev. B **63**, 054529 (2001).
[10] J. L. Sarrao and J. D. Thompson, J. Phys. Soc. Jpn. **76**, 051013 (2007).
[11] J. Thompson, R. Movshovich, Z. Fisk, F. Bouquet, N. Curro, R. Fisher, P. Hammel, H. Hegger, M. Hundley, M. Jaime, P. Pagliuso, C. Petrovic, N. Phillips, and J. Sarrao, J. Magn. Magn. Mater. **226–230**, 5 (2001).
[12] H. Shishido, R. Settai, D. Aoki, S. Ikeda, H. Nakawaki, N. Nakamura, T. Iizuka, Y. Inada, K. Sugiyama, T. Takeuchi, K. Kindo, T. C. Kobayashi, Y. Haga, H. Harima, Y. Aoki, T. Namiki, H. Sato, and Y. Ōnuki, J. Phys. Soc. Jpn. **71**, 162 (2002).
[13] G. F. Chen, K. Matsubayashi, S. Ban, K. Deguchi, and N. K. Sato, Phys. Rev. Lett. **97**, 017005 (2006).
[14] G. Knebel, D. Aoki, D. Braithwaite, B. Salce, and J. Flouquet, Phys. Rev. B **74**, 020501 (2006).
[15] G. Knebel, D. Aoki, J.-P. Brison, L. Howald, G. Lapertot, J. Panarin, S. Raymond, and J. Flouquet, Phys. Status Solidi B **247**, 557 (2010).
[16] T. Park, M. J. Graf, L. Boulaevskii, J. L. Sarrao, and J. D. Thompson, Proc. Natl. Acad. Sci. USA **105**, 6825 (2008).
[17] S. Nair, O. Stockert, U. Witte, M. Nicklas, R. Schedler, K. Kiefer, J. D. Thompson, A. D. Bianchi, Z. Fisk, S. Wirth, and F. Steglich, Proc. Natl. Acad. Sci. USA **107**, 9537 (2010).
[18] R. R. Urbano, B.-L. Young, N. J. Curro, J. D. Thompson, L. D. Pham, and Z. Fisk, Phys. Rev. Lett. **99**, 146402 (2007).
[19] N. Kimura, K. Ito, K. Saitoh, Y. Umeda, H. Aoki, and T. Terashima, Phys. Rev. Lett. **95**, 247004 (2005).
[20] N. Fukushima, Phys. Rev. B **78**, 115105 (2008).
[21] P. D. Sacramento, J. Phys. Condens. Matter **15**, 6285 (2003).
[22] H. Tsunetsugu, M. Sigrist, and K. Ueda, Rev. Mod. Phys. **69**, 809 (1997).
[23] J. V. Alvarez and F. Yndurain, Phys. Rev. Lett. **98**, 126406 (2007).
[24] Y. Yanase and M. Sigrist, J. Phys. Soc. Jpn. **78**, 114715 (2009).
[25] A. Aperis, G. Varelogiannis, and P. B. Littlewood, Phys. Rev. Lett. **104**, 216403 (2010).
[26] J. Spałek, Phys. Rev. B **38**, 208 (1988).
[27] M. M. Maśka, M. Mierzejewski, J. Kaczmarczyk, and J. Spałek, Phys. Rev. B **82**, 054509 (2010).
[28] For the discussion of various forms of t-J model, see Ref. 48 below.
[29] K. A. Chao, J. Spalek, and A. M. Oles, J. Phys. C **10**, L271 (1977).
[30] F. C. Zhang and T. M. Rice, Phys. Rev. B **37**, 3759 (1988).
[31] A. Moreno, A. Muramatsu, and S. R. Manmana, Phys. Rev. B **83**, 205113 (2011).
[32] K. Maki, Phys. Rev. **148**, 362 (1966).
[33] K. Kumagai, M. Saitoh, T. Oyaizu, Y. Furukawa, S. Takashima, M. Nohara, H. Takagi, and Y. Matsuda, Phys. Rev. Lett. **97**, 227002 (2006).
[34] P. W. Anderson, P. A. Lee, M. Randeria, T. M. Rice, N. Trivedi, and F. C. Zhang, J. Phys. Condens. Matter **16**, R755 (2004).
[35] J. Bünemann, T. Schickling, and F. Gebhard, e-print arXiv:1108.4284.
[36] N. Fukushima, J. Phys. A: Math. Theor. **44**, 075002 (2011).

[37]P. Fazekas, *Lecture Notes on Electron Correlation and Magnetism* (World Scientific Publishing, 1999), Chap. 7.
[38]M. Ogata and H. Fukuyama, Rep. Prog. Phys. **71**, 036501 (2008).
[39]B. Kyung, Phys. Rev. B **62**, 9083 (2000).
[40]G. C. Psaltakis and E. W. Fenton, J. Phys. C **16**, 3913 (1983).
[41]S. Tsonis, P. Kotetes, G. Varelogiannis, and P. B. Littlewood, J. Phys. Condens. Matter **20**, 434234 (2008).
[42]P. Fulde and R. A. Ferrell, Phys. Rev. **135**, A550 (1964).
[43]A. Larkin and Y. Ovchinnikov, J. Exp. Theor. Phys. **47**, 1136 (1964); Sov. Phys. JETP **20**, 762 (1965).
[44]Y. Matsuda and H. Shimahara, J. Phys. Soc. Jpn. **76**, 051005 (2007).
[45]M. Ogata, J. Phys. Soc. Jpn. **66**, 3375 (1997).
[46]F. Loder, A. P. Kampf, and T. Kopp, Phys. Rev. B **81**, 020511 (2010).
[47]A. Ptok, M. M. Maśka, and M. Mierzejewski, J. Phys. Condens. Matter **21**, 295601 (2009).
[48]J. Jędrak and J. Spałek, Phys. Rev. B **83**, 104512 (2011).
[49]J. Jędrak and J. Spałek, Phys. Rev. B **81**, 073108 (2010).
[50]J. Kaczmarczyk, J. Jędrak, and J. Spałek, Acta Phys. Pol. A **118**, 261 (2010).
[51] J. Jędrak, J. Kaczmarczyk, and J. Spałek, e-print arXiv:1008.0021 (unpublished).
[52]Q.-H. Wang, Z. D. Wang, Y. Chen, and F. C. Zhang, Phys. Rev. B **73**, 092507 (2006).
[53]K.-Y. Yang, W. Q. Chen, T. M. Rice, M. Sigrist, and F.-C. Zhang, New J. Phys. **11**, 055053 (2009).
[54]J. Kaczmarczyk and J. Spałek, Phys. Rev. B **79**, 214519 (2009).
[55]J. Kaczmarczyk and J. Spałek, J. Phys. Condens. Matter **22**, 355702 (2010).
[56]P. Korbel, J. Spałek, W. Wójcik, and M. Acquarone, Phys. Rev. B **52**, R2213 (1995).
[57]G. Kotliar and A. E. Ruckenstein, Phys. Rev. Lett. **57**, 1362 (1986).
[58]J. Spałek and W. Wójcik, *Spectroscopy of the Mott Insulators and Correlated Metals*, edited by A. Fujimori and Y. Tokura (Springer-Verlag, Berlin, 1995), Vol. 119, pp. 41–65.
[59]M. Galassi, J. Davies, J. Theiler, B. Gough, G. Jungman, P. Alken, M. Booth, and F. Rossi, *GNU Scientific Library Reference Manual*, 3rd ed. (Network Theory, Ltd., London, 2009).
[60]J. Kaczmarczyk, Ph. D. Thesis, Jagiellonian University, Kraków, 2011 [http://th-www.if.uj.edu.pl/ztms/download/phdTheses/Jan_Kaczmarczyk_doktorat.pdf].
[61]T. Koretsune and M. Ogata, Phys. Rev. Lett. **89**, 116401 (2002).
[62]T. Koretsune and M. Ogata, J. Phys. Soc. Jpn. **72**, 2437 (2003).
[63]W. O. Putikka, M. U. Luchini, and M. Ogata, Phys. Rev. Lett. **69**, 2288 (1992).
[64]M. Raczkowski, D. Poilblanc, R. Frésard, and A. M. Oleś, Phys. Rev. B **75**, 094505 (2007).
[65]M. Ogata and A. Himeda, J. Phys. Soc. Jpn. **72**, 374 (2003).
[66]Although in $CeRhSi_3$ the phases have only been analyzed as a function of temperature.
[67]A. Himeda and M. Ogata, Phys. Rev. B **60**, R9935 (1999).
[68]T. Giamarchi and C. Lhuillier, Phys. Rev. B **43**, 12943 (1991).
[69]M. Inaba, H. Matsukawa, M. Saitoh, and H. Fukuyama, Physica C **257**, 299 (1996).
[70]O. Howczak, Ph. D. Thesis, Jagiellonian University, Kraków, in preparation.